Annals of Anatomy 206 (2016) 27–33

Contents lists available at ScienceDirect

Annals of Anatomy

journal homepage: www.elsevier.com/locate/aanat

Methods

Preparation of human formalin-fixed brain slices for electron microscopic investigations

Martin Krause[a], Martin Brüne[b], Carsten Theiss[a,*]

[a] Institute of Anatomy, Department of Cytology, Ruhr-University Bochum, Germany
[b] LWL University Hospital Bochum, Division of Cognitive Neuropsychiatry and Psychiatric Preventive Medicine, Ruhr-University Bochum, Germany

ARTICLE INFO

Article history:
Received 18 December 2015
Received in revised form 13 April 2016
Accepted 15 April 2016

Keywords:
Human formalin fixed brain slices
Post mortem tissue
Electron microscopy
Ultrastructure, Von Economo Neuron
Schizophrenia

ABSTRACT

Ultra-structural analysis of human post-mortem brain tissue is important for investigations into the pathomechanism of neuropsychiatric disorders, especially those lacking alternative models of studying human-specific morphological features. For example, Von Economo Neurons (VENs) mainly located in the anterior cingulate cortex and in the anterior part of the insula, which seem to play a role in a variety of neuropsychiatric conditions, including frontotemporal dementia, autism and schizophrenia, can hardly be studied in nonhuman animals. Accordingly, little is known about the ultra-structural alterations of these neurons, though important research using qualitative stereological methods has revealed that protein expression of the VENs assigns them a role in immune function.

Formaldehyde, which is the most common fixative in human pathology, interferes with the immunoreactivity of the tissue, possibly leading to unreliable results. Therefore, a method for ultra-structural investigations independent of antigenic properties of the fixated tissue is needed. Here, we propose an approach using electron microscopy to examine cytoskeletal structures, synapses and mitochondria in these cells. We also show that our methodology is able to keep tissue consumption to a minimum, while still allowing for the specimens to be handled with ease by using agar embedded slices in contrast to blocks for the embedding procedure. Accordingly, a stepwise protocol utilising 60 μm thick human post mortem brain sections for electron microscopic ultra-structural investigations is presented.

1. Introduction

For morphological investigations of psychiatric disorders, human post-mortem neuronal tissue is of great interest. While empirical research on the malfunctions of these disorders at the cellular level is limited, there is a need to develop novel tools to study the morphology and ultrastructure of neuronal tissue. Such studies could improve our understanding of the cellular pathology of neuropsychiatric disorders, and ultimately help develop more targeted therapeutic strategies.

Recently, disrupted in schizophrenia 1 (DISC1) has become a focus of neuropsychiatric disorder investigations. This gene was first described in a Scottish pedigree suffering several psychiatric disorders such as schizophrenia, schizoaffective disorder, uni- and bipolar affective disorder. In this family, DISC1 is disrupted by a balanced translocation (Millar et al., 2000). DISC1 is located within the cytoplasm as well as in the nucleus and provides a wide range of different cellular functions through interactions with other proteins, such as neuronal migration, cell proliferation during development of the nervous system (Ishizuka et al., 2011; Kamiya et al., 2005), neurite outgrowth (Miyoshi et al., 2003; Ozeki et al., 2003), dendritic spine regulation (Hayashi-Takagi et al., 2010), microtubule organisation and finally interaction with microtubule transport proteins (Kamiya et al., 2005). DISC1 is also involved in vesicle transport processes, and in the case of an impaired DISC1 function, the transport mechanisms can be restored using lithium as a therapeutic strategy (Flores et al., 2011). The different functions of DISC1 are well established by immunohistochemistry, but data on ultra-structural alterations is missing.

The alteration of cellular structures is a common theme across many neuropsychiatric disorders. In patients with schizophrenia who predominantly display positive symptoms such as delusions or hallucinations, damaged myelinated fibres in the grey matter can be found. Conversely, in patients with predominantly negative symptoms such as emotional blunting, a degeneration of myelinated sheaths in the white matter is detectable (Uranova et al., 2011). Additionally, patients with schizophrenia suffer a loss of dendrites

* Corresponding author at: Ruhr-University Bochum, Universitätsstraße 150, MA 5/47, 44780 Bochum, Germany. Tel.: +49 234 32 26733; fax: +49 234 32 14476.
E-mail address: carsten.theiss@rub.de (C. Theiss).

http://dx.doi.org/10.1016/j.aanat.2016.04.030
0940-9602/

in layer III and V pyramidal cells of the medial prefrontal cortex, and a decreased basilar dendritic spine density of the pyramidal cells of layer III in the dorsolateral prefrontal cortex (Broadbelt et al., 2002; Glantz and Lewis, 2000; reviewed in Kulkarni and Firestein, 2012).

Electron microscopy allows us to obtain a clear depiction of all cell organelles and the cytoskeleton. However, this technique depends on certain prerequisites concerning the fixation protocol, with the best results being obtained for ultra-structural analysis by using glutaraldehyde as a fixative. At the beginning of the electron microscopy era, several aldehydes where tested and used as a fixative in electron microscopic investigations (Sabatini et al., 1963). Today, mostly a combination of glutaraldehyde and paraformaldehyde is used for tissue fixation (Bando et al., 2015; Freiman et al., 2002; Lim et al., 1997). In addition, fixation using only formaldehyde (Wadsworth et al., 1995) or glutaraldehyde (Zhang et al., 2015) has also been performed.

In human pathology, the specimens are typically fixed in formaldehyde (Gomez-Nicola et al., 2014; Hales et al., 2014), which might influence the protein-antigenicity (O'Leary et al., 2009) and thus immunohistochemical results may be unreliable. Furthermore, in most cases, the post-mortem interval until the fixative penetrates the tissue is substantially higher in human pathology compared to tissue fixation of laboratory animals. During this critical period, the tissue may disintegrate and lose its antigenicity. Because of these aspects, an antigenicity independent method such as electron microscopy is necessary for the examination of intracellular structures.

The embedding procedure described by Luft in 1961 has not undergone substantive changes until now (Luft, 1961). This approach is perfectly applicable for tissue blocks, but reveals deficits in the handling of sections. To address this, we add an agar pre-embedding step.

Accordingly, we here present a protocol that allows us to investigate individual neurons in human post-mortem brain tissue at the ultra-structural level. As an example, we show the ultra-structural characteristics of Von Economo Neurons (VENs), that are putatively involved in the pathomechanisms of neurodegenerative and psychiatric disorders (Allman et al., 2001; Von Economo, 1926). Furthermore, nearly all VENs are DISC1 positive in contrast to pyramidal cells of the same layer (Allman et al., 2011). VENs cannot be found in common laboratory animals such as rodents (Raghanti et al., 2015). Thus, an alternative is to examine these neurons in the post-mortem tissue of body donors who suffered from these disorders. While a common approach is the use of tissue blocks for electron microscopic investigations, we aim to demonstrate that the utilisation of agar pre-embedded brain slices is much easier, more economical and can help save precious tissue resources.

2. Materials and methods

2.1. Material

For the following protocol we used 60 μm thick coronal plane cryoprotected sections of the human anterior cingulate cortex (ACC) obtained from the Stanley Foundation Neuropathology Consortium (SFNC; Chevy Chase, USA). The study was approved by the Ethics Committee of the Medical Faculty of the Ruhr-University Bochum, Germany.

The human post-mortem brains were made available to the SFNC with a post mortem interval of 18–50 h, and then fixed in formaldehyde for several weeks, stepwise transferred into a sucrose solution and finally stored in a 30% sucrose buffer for cryoprotection, before they were cut into sections.

2.2. Material preparation

The cryoprotected ACC slices were transferred into a petri dish with phosphate buffered saline (PBS; Fig. 1A) and subdivided into five different parts (Fig. 1B and C), to diminish consumption of the post-mortem human brain tissue. For our study, the region of interest is located at the top of the ACC gyrus; therefore, we used part B for the electron microscopic investigations. Finally, the selected part B is subdivided again into approximately 1 mm wide strips to get the specimen ready for embedding (Fig. 1D).

2.3. Embedding

For the embedding process, which takes three days followed by two days of epoxy resin hardening, we use a slightly modified embedding protocol described by John H. Luft (Luft, 1961). On the first day, the specimens were rinsed in phosphate buffer (PB; Fig. 1E) three times, 10 min at each step. The tissue was then placed in Dalton solution for 2 h (Fig. 1F). Following this, we embed the slice into an agar block (Fig. 1G) to not only improve the handling of the sections, but also to prevent the specimens from contorting during dehydration. The Dalton solution is a mixture of 25 ml 5% potassium dichromate, 25 ml 3.4% sodium chloride, 50 ml distilled water and 1 g osmium tetra-oxide. For the required pH value of 7.4, a 2.5 N potassium hydroxide solution was used. After incubation in Dalton solution, the tissue was washed three times in PB for 10 min each. Next, the specimens were dehydrated through an ascending ethanol series (Fig. 1H). Dehydration started with 50%-ethanol for 15 min, followed by incubation in a 70%-ethanol, 1%-uranyl acetate and 1%-phosphotungstic acid solution over night at 4 °C. The next day, dehydration continued with 70%-ethanol (15 min), 80%-ethanol (15 min), 90%-ethanol (15 min), 95%-ethanol (15 min) and finally three steps in 100%-ethanol (15 min). After this, the specimens were carefully transferred into epoxy resin (Fig. 1I). This was accomplished by first incubating the tissue in propylene oxide for 20 min, followed by an ascending series of propylene oxide and EPON mixtures (glycid ether 100 = EPON 812 4.85 ml, 2-dodecenylsuccinic acid anhydride = DDSA 1.85 ml, methylnadic anhydride = MNA 3.3 ml, 2,4,6-tris(dimethylaminomethyl)phenol = DMP-30 0.15 ml). This embedding procedure started with propylene oxide/EPON in a 3:1 ratio for 45 min, followed by a 1:1 ratio for 1 h, and ended with a 1:3 ratio for 2 h. This ascending series of propylene oxide and EPON mixture also differs from the original protocol and induces a slow and thorough replacement of the alcohol by EPON. Finally, specimens were penetrated by pure EPON over night at 20 °C (Fig. 1J). On the third day of embedding, EPON was renewed for a better tissue infiltration for an additional 2 h. This was done after casting in a mould together with an embedding number to simplify the cataloguing of the specimen. Finally, the EPON embedded specimen was allowed to polymerise at 60 °C for two days (Fig. 1K and L).

2.4. Cutting

Before the EPON pyramids were ready for semi- and ultrathin cutting, they had to be trimmed in a preparatory step with a Leica EM TRIM (Leica Microsystems GmbH, Wetzlar, Germany). During this step it was necessary to trim the pyramid into a trapezoid-shape very close to the edge of the specimen. The smallest possible cutting area better facilitated the subsequent handling steps.

Another preparatory step was the preparation of Formvar-coated grids. Therefore, Formvar was dissolved in chloroform to get a 0.3% solution. A thoroughly cleaned object slide was dipped into the Formvar solution and smoothly pulled up to get a uniform Formvar film on the object slide. When the Formvar had dried completely, the film had to be carved near the object slide edges

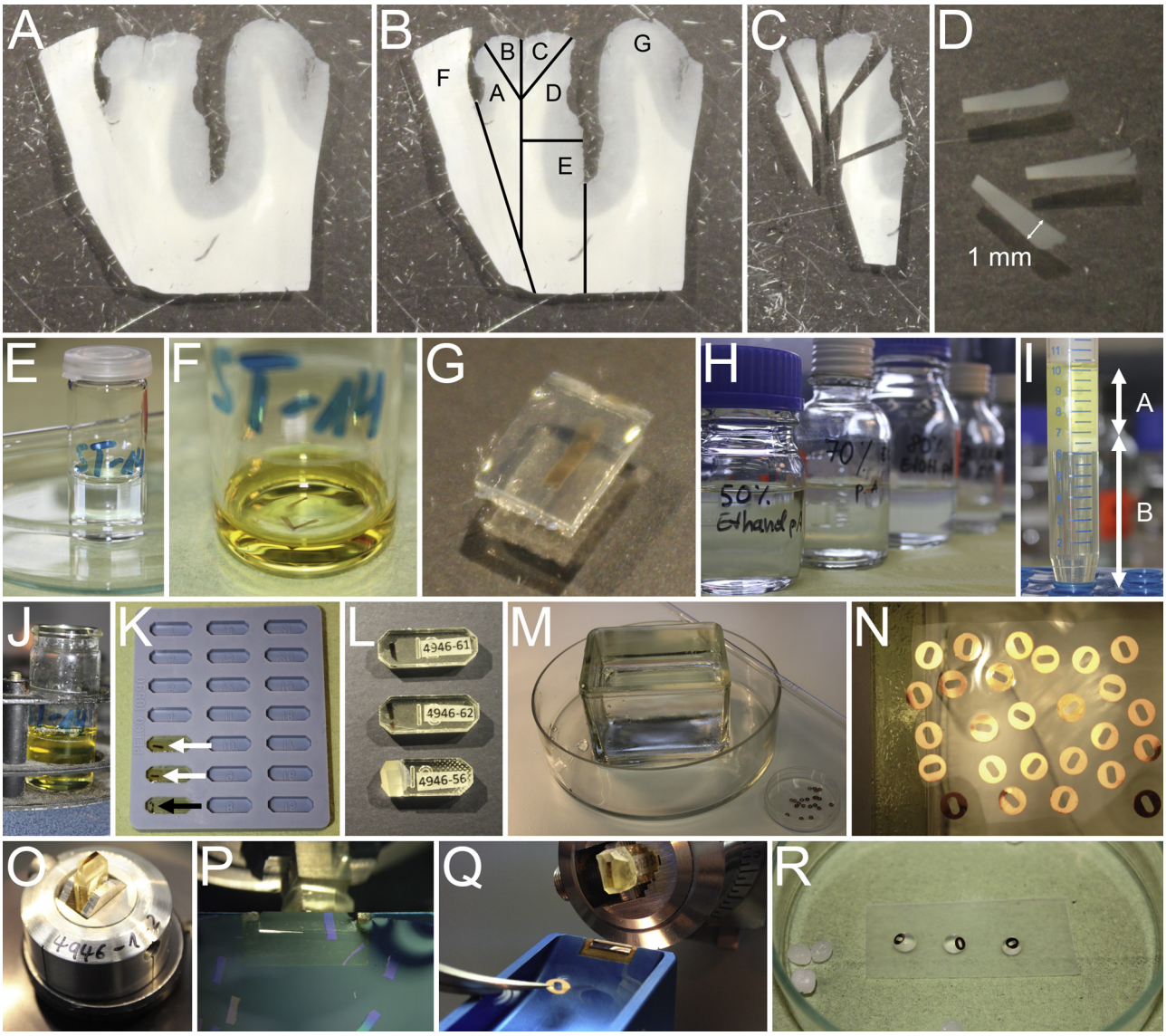

Fig. 1. 60 μm thick coronal brain slices from the ACC were cut into five different parts (A–C), part B was then subdivided into 1 mm wide strips for the EM embedding (D). After the tissue is thoroughly rinsed in PB (E), the specimen is incubated in Dalton solution (F), embedded in an agar block (G) and dehydrated in an ascending ethanol series (H). For the final EPON mixture, a 3:7 ratio of EPON solution A and B is necessary (I), before the tissue is incubated in pure EPON over night (J), followed by polymerisation (K). It is also clearly visible that the agar embedded slices come through the embedding procedure unscathed (white arrows), whereas the non-agar-protected slice broke into three parts (black arrow). After hardening, the pyramids have to be trimmed to prepare them for cutting (L). A tank is filled to the brim with water (M) to create a surface free of dust for placing grids on a Formvar film (N). If an ideal layer is found within a semithin section (O and P), the ultrathin slice is fished onto a Formvar-coated copper grid (Q) and contrasted with lead citrate (R).

with a sharp knife. Next, the object slide was dipped slowly into distilled water in a 45° angle, so that the Formvar film detached from the object slide and floated on the water surface. Copper grids (2 mm × 1 mm slot, ∅ 3.05 mm; agar scientific, AGG2500 C) were placed carefully on the Formvar film with their dull side facing the film. With Parafilm® M, the grid mounted Formvar film could be picked up from the water and placed in a petri dish for drying and storage (Fig. 1M and N).

The semi- and ultrathin slices were cut with an Ultracut E Reichert-Jung (Leica Microsystems GmbH, Wetzlar, Germany). First, semithin slices (thickness of 0.5 μm; Fig. 1O and P) were made with a DiATOME histo diamond knife (45°, 6 mm, MX559; Diatome AG, Biel, Switzerland), and then ultrathin slices (thickness of 60 nm) were cut with a DiATOME ultra diamond knife (45°, 2,1 mm, MX3716; Diatome AG, Biel, Switzerland).

Because of the thin sections of raw material, cutting for ultrastructural investigation was carried out very carefully, so as not to miss the perfect slice. For instance, in the present protocol it was essential to characterise VENs in layer V of the neocortex based on their characteristic morphology. Therefore, we picked up the semi-sections and stained them with methyleneblue-azur II (Richardson et al., 1960) to identify the VENs. For ultrathin slices of VENs, diamond knives were used, and sections were placed on prepared Formvar-coated grids (Fig. 1Q) and contrasted with Reynolds' lead citrate (Reynolds, 1963; Fig. 1R).

2.5. Localisation of the VENs

To identify VENs in semithin cuts, an Olympus BX61VS microscope (Olympus, Shinjuku, Japan) equipped with an UPlan SApo 40x/0.95 objective (Olympus, Shinjuku, Japan) was used. The digital micrographs were taken with VS-ASW 2.6 (Virtual Slide System multi slide) (Olympus Soft Imaging Solutions GmbH, Münster, Germany). Specifically, we stained every tenth semithin slice and

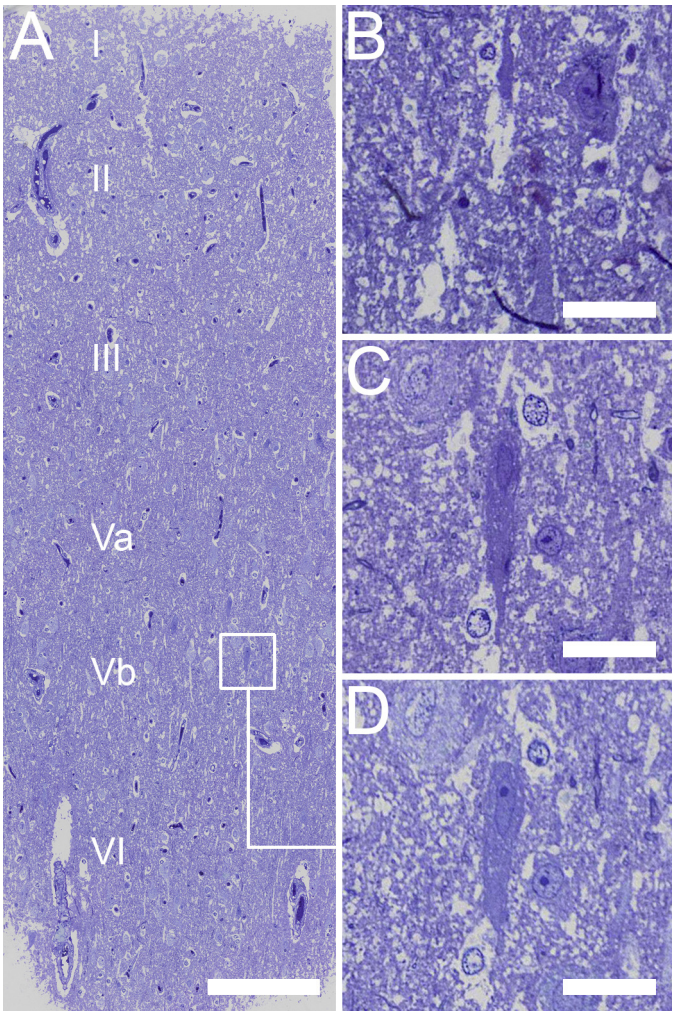

Fig. 2. If a region of interest is detected in layer Vb of the ACC (A) consecutive slices are stained (B and C) to find an ideal section, characterised by a spindle shaped VEN with a visible nucleus and nucleolus (D). Scale bars: A = 200 μm; B–D = 25 μm.

checked the region of interest (Fig. 2A). Once the region of interest was identified, each fifth slice was picked up, stained and screened for VENs (Fig. 2B and C). As soon as a Von Economo Neuron (VEN) appeared, every slice was stained to find an ideal section of this VEN, clearly identified by the nucleus plus visible nucleolus (Fig. 2D). Furthermore, it is very helpful to screen the whole section for other landmarks such as blood vessels, and keep their relation to VENs in mind. This was done to aid with orientation later at the electron microscope, making locating the selected VEN much easier and more time-efficient.

2.6. Electron microscopy

The contrasted grids were analysed utilising a Philips EM 420 (Philips, Amsterdam, Netherlands) transmission electron microscope equipped with a digital CCD camera (Model 792 BioScan; Gatan, Pleasanton, USA) and a Ditabis Micron System for photographic plates (DITABIS Digital Biomedical Imaging Systems AG, Pforzheim, Germany). In our study, the specimens were magnified 10,500-fold and 82,000-fold at 80 kV to get a clear depiction of the cell organelles. While it is possible to use higher magnifications with this formaldehyde treated human post-mortem brain tissue, for the purpose of our examination it was necessary to get a complete image of each examined cell. Thus, the entire cell was screened and photographed, the images were later collaged with Adobe Photoshop CS 6 (Adobe Systems Incorporated, San Jose, USA) and then measured with ImageJ 1.47 (Schneider et al., 2012). Due to the three-dimensionality of neurons and their cell organelles, we captured each cell in up to four different sections and arithmetically averaged the data.

3. Results and discussion

In human pathology, the post-mortem interval is a relevant factor for tissue preservation. It is known that degenerative alterations in the cytoplasm of glial cells and within the axoplasm can occur within 24 h at 4 °C, and especially mitochondria are known to be vulnerable to degeneration. The same degenerative effects already appear after 6 h at a storage temperature of 25 °C (Hukkanen and Röyttä, 1987). In our study, the tissue had a mean post-mortem interval of 31.89 ± 9.649 h and showed the typical ultra-structural alterations of network-like splitting of the inner part of the myelin sheath (Fig. 3A), as described by Hukkanen and Röyttä (1987). However, other structures such as microtubules, neurofilaments, synapses, vesicles and mitochondria were well preserved (Fig. 3B–D). In particular, entire neurons such as VENs, which are currently of most interest in investigations of psychiatric disorders, could be depicted clearly in a collage of merged micrographs (Fig. 3E).

The most common fixative in human pathology is formaldehyde. Its tissue penetration speed averages from 0.5 to 1 mm/h and so the post-mortem interval is additively extended until the fixation process is completed. However, formaldehyde stabilises the secondary structure of proteins and makes them thermo-stable against high temperatures (Mason and O'Leary, 1991). Unfortunately, the intra- and intermolecular cross-linking that confers this thermo-stability also results in a decreased immunoreactivity of the tissue (Rait et al., 2004). For human post-mortem brain tissue that has been treated with formaldehyde for several weeks, it can be assumed that the antigenicity is affected, and that any immunohistochemical results may be unreliable. Hence, electron microscopic investigations are an alternative option for conducting detailed morphological ultra-structural examinations.

Other critical aspects of tissue preservation include the storage time and method. In human pathology and investigations of neuropsychiatric diseases, the tissue is collected over a longer period of time and has to be stored until the study begins. There are basically two options for storing the specimen over a long period: on the one hand, long-term fixation in formaldehyde, and on the other hand, freezing the cryoprotected tissue. Both methods seem to be equal concerning tissue preservation (Liu and Schumann, 2014) and the important factor is presumably the post-mortem interval.

Summarising, in ultra-structural studies on human post-mortem tissue it is more important to use tissue with similar post-mortem intervals than similar storage times. Furthermore, it is possible to undertake ultra-structural investigations on specimens with high post-mortem intervals above 24 h.

A main difference between our approach and the common tissue embedding protocol for electron microscopy is the utilisation of tissue sections in contrast to tissue blocks. Such blocks should have an edge length of 1 mm, which leads to higher tissue consumption. To save tissue we used 60 μm thick cryosections, which led to a reduction in tissue consumption by 94%.

Since epoxy resin hardening causes the tissue to sink, it becomes located at the pyramid sidewall, making it necessary to cut off the upper part of the pyramid, turning it 90° and then glueing the two fragments together with epoxy resin. Here it is important to make sure that the different pyramid fragments are not interchanged. The best option for preventing such an error is to

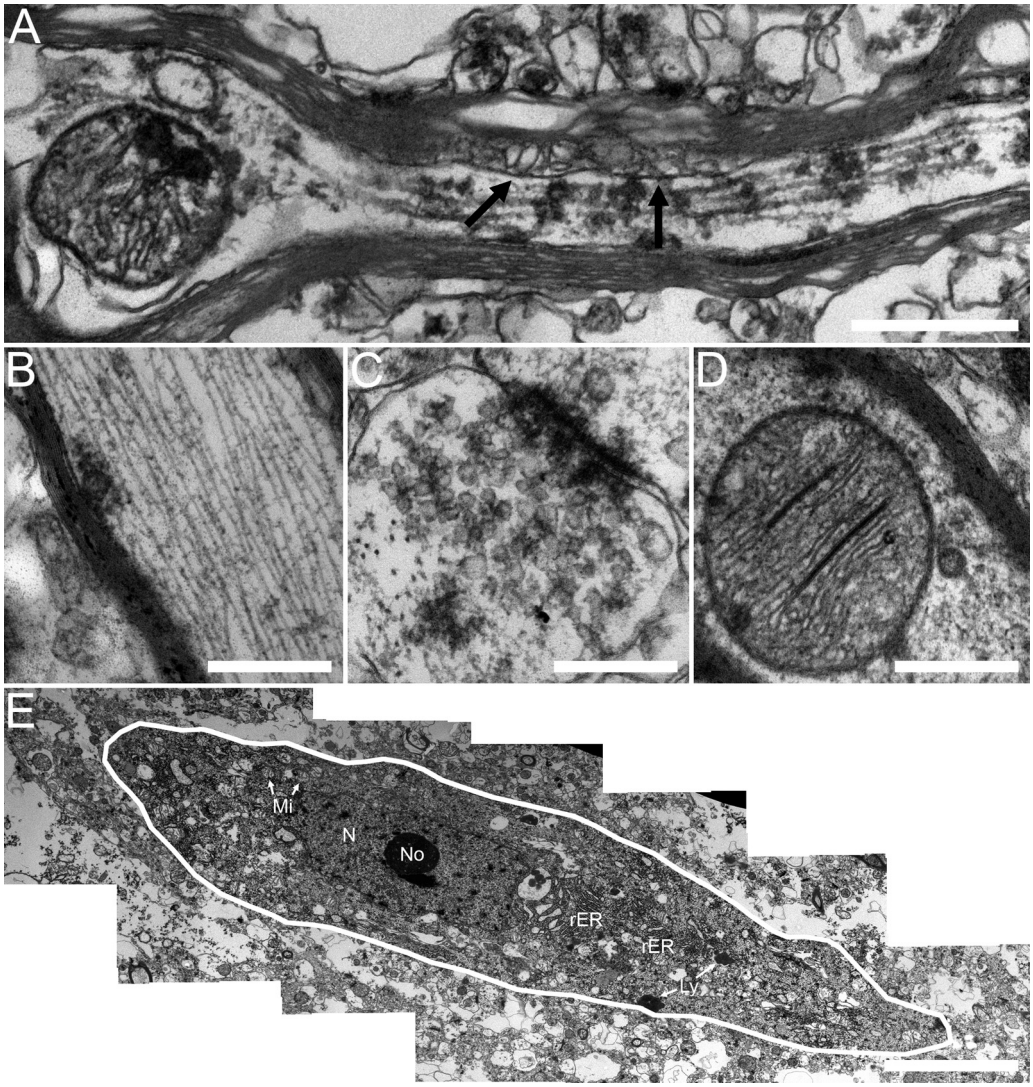

Fig. 3. (A) Electron microscopic picture of an axon with microtubules, mitochondria and a network-like splitting of the inner part of the myelin sheath (arrows). (B) Neurofilaments, (C) chemical synapses with numerous presynaptic vesicles, (D) and mitochondria are well preserved. (E) Photomontages of entire neurons like VENs could be used to estimate the amount and localisation of different cell organelles (N = nucleus; No = nucleolus; rER = rough endoplasmatic reticulum; Mi = mitochondria; Ly = lysosomes). Scale bars: A = 500 nm; B–D = 350 nm; E = 7000 nm.

rearrange the pyramids gradually. Unfortunately, the sections tend to contort slightly during the dehydration process, which makes the cutting process more precarious. Although it is possible to cut these pyramids if the region of interest is correctly positioned into the ultra-microtome, it is helpful to pre-embed the section in an agar block to gain two advantages: Firstly, the section is protected against warping during dehydration (Fig. 1K white arrows), which simplifies the cutting process and the identification of different layers of neocortex. Secondly, after the dehydration process, the slices that were not protected by agar embedding are very fragile and tend to break into pieces between embedding steps during transfer (Fig. 1K black arrow). Thus, the handling of slices becomes easier by embedding them in an agar block. Regardless of whether the slices are pre-embedded in an agar block or not, it is a good idea to mark either the pial surface or the white matter by a diagonal cut through the pyramid to have a better orientation to identify the region of interest.

Because of the necessity to analyse the entire cell network in order to distinguish the different layers of the neocortex to identify the region of interest, we used single hole grids. This allows us to find all previously noted landmarks that guide us to the VENs.

With the method presented here, it is possible to identify a specific single neuron in an intact cell network under the electron microscope in a very time-efficient manner. In addition, this method allows for detecting the same neuron in different ultra-thin slices, with the aim of getting better insights into the three-dimensionality of neurons.

To avoid ripping of the Formvar film, the electron beam intensity should be decreased to a low level, so that the energy at a single point within the specimen is reduced to a minimum. Besides this, if possible, the specimen should be cooled and the exposure time reduced to a minimum.

Since 1949, when Egaz Moniz received the Noble Price for his lobotomy procedure as a treatment for severe psychiatric disorders (Diefenbach et al., 1999), both knowledge and treatment options have dramatically changed. In the decades since, it has been discovered that many mental disorders are characterised by subtle, rather than gross morphological alterations involving diverse structures of the central nervous system. With regards to VENs, frontotemporal dementia is associated with a VEN loss of 74% (Seeley et al., 2006). In Alzheimer's disease, especially in later stages, VEN degeneration of 60% is detectable (Nimchinsky et al., 1995). There is also

evidence to suggest that VENs are pathologically altered in autism (Simms et al., 2009) and schizophrenia (Brüne et al., 2010), and it is possible that VENs are somehow linked to complex behaviours such as suicide (Brüne et al., 2011). Conversely, a higher density of VENs in the ACC has been found in "Super agers", elder people with exceptionally preserved memory capacities (Gefen et al., 2015). We suggest that aside from the classical microscopic analyses of protein expression (Cobos and Seeley, 2015; Stimpson et al., 2011) and dendritic architecture (Watson et al., 2006), ultra-structural investigations of neurons can help identify the pathomechanisms of neuropsychiatric disorders, as exemplified by the examination of VENs.

4. Conclusion

The present protocol provides researchers with the option to investigate formaldehyde-fixed human post-mortem brain tissue on an ultra-structural level. As pointed out, this technique is ideal for morphometric studies of highly valuable material, by reducing tissue consumption to a minimum while simultaneously keeping the handling of tissue manageable. We believe that this approach may open new avenues to improve our understanding of complex neuropsychiatric diseases.

Acknowledgments

The authors would like to thank C. Grzelak and A. Lodwig for their excellent technical assistance, but also A. Lenz for her secretarial work. Furthermore, we are grateful to D. Terheyden-Keighley for proof reading.

Appendix A.

A blank embedding protocol sheet for your own work is available in the online version (Table 1).

Table 1
Step by step protocol for EPON embedding of formalin fixed human brain slices.

Project description	Embedding number	
Step	For	Check box
Day 1		
Rinse specimen in PB (3×)	10 min	
Dalton	2 h	
Rinse specimen in PB (3×)	10 min	
Ethanol 50%	15 min	
Ethanol 70%		
+ 1% uranyl acetate + 1% phosphotungstic acid	Over night at 4 °C	
Day 2		
Ethanol 70%	15 min	
Ethanol 80%	15 min	
Ethanol 90%	15 min	
Ethanol 95%	15 min	
Ethanol 100% (3×)	15 min	
Propylene oxide	20 min	
Propylene oxide/EPON – 3:1 ratio	45 min	
Propylene oxide/EPON – 1:1 ratio	1 h	
Propylene oxide/EPON – 1:3 ratio	2 h	
Pure EPON	Over night at 20 °C	
Day 3		
Pure EPON (renewed)	2 h	
Transfer specimen in a mould		
Hardening in an incubator	2 days at 60 °C	

EPON making:
Solution A: EPON 812 (62 ml) + DDSA (100 ml).
Solution B: EPON 812 (100 ml) + MNA (89 ml).
EPON: Solution A (3 ml) + Solution B (7 ml) + DMP-30 (0.15 ml).
[Each has to be mixed until the solution is homogenous.]
Notice: For 1 specimen embedding approximately 10 ml EPON are required.

Appendix B. Supplementary data

Supplementary material related to this article can be found, in the online version, at http://dx.doi.org/10.1016/j.aanat.2016.04.030.

References

Allman, J.M., Hakeem, A., Erwin, J.M., Nimchinsky, E., Hof, P., 2001. The anterior cingulate cortex. The evolution of an interface between emotion and cognition. Ann. N. Y. Acad. Sci. 935, 107–117, http://dx.doi.org/10.1111/j.1749-6632.2001.tb03476.x.

Allman, J.M., Tetreault, N.A., Hakeem, A.Y., Manaye, K.F., Semendeferi, K., Erwin, J.M., Park, S., Goubert, V., Hof, P.R., 2011. The von Economo neurons in the frontoinsular and anterior cingulate cortex. Ann. N. Y. Acad. Sci. 1225, 59–71, http://dx.doi.org/10.1111/j.1749-6632.2011.06011.x.

Bando, Y., Nomura, T., Bochimoto, H., Murakami, K., Tanaka, T., Watanabe, T., Yoshida, S., 2015. Abnormal morphology of myelin and axon pathology in murine models of multiple sclerosis. Neurochem. Int. 81, 16–27, http://dx.doi.org/10.1016/j.neuint.2015.01.002.

Broadbelt, K., Byne, W., Jones, L.B., 2002. Evidence for a decrease in basilar dendrites of pyramidal cells in schizophrenic medial prefrontal cortex. Schizophr. Res. 58, 75–81, http://dx.doi.org/10.1016/S0920-9964(02)00201-3.

Brüne, M., Schöbel, A., Karau, R., Benali, A., Faustmann, P.M., Juckel, G., Petrasch-Parwez, E., 2010. Von Economo neuron density in the anterior cingulate cortex is reduced in early onset schizophrenia. Acta Neuropathol. 119, 771–778, http://dx.doi.org/10.1007/s00401-010-0673-2.

Brüne, M., Schöbel, A., Karau, R., Faustmann, P.M., Dermietzel, R., Juckel, G., Petrasch-Parwez, E., 2011. Neuroanatomical correlates of suicide in psychosis: the possible role of von Economo Neurons. PLoS ONE 6, e20936, http://dx.doi.org/10.1371/journal.pone.0020936.

Cobos, I., Seeley, W.W., 2015. Human von Economo Neurons express transcription factors associated with layer V subcerebral projection neurons. Cereb. Cortex 25, 213–220, http://dx.doi.org/10.1093/cercor/bht219.

Diefenbach, G.J., Diefenbach, D., Baumeister, A., West, M., 1999. Portrayal of lobotomy in the popular press: 1935–1960. J. Hist. Neurosci. 8, 60–69, http://dx.doi.org/10.1076/jhin.8.1.60.1766.

Flores, R., Hirota, Y., Armstrong, B., Sawa, A., Tomoda, T., 2011. DISC1 regulates synaptic vesicle transport via a lithium-sensitive pathway. Neurosci. Res. 71, 71–77, http://dx.doi.org/10.1016/j.neures.2011.05.014.

Freiman, T.M., Gimbel, K., Honegger, J., Volk, B., Zentner, J., Frotscher, M., Deller, T., 2002. Anterograde tracing of human hippocampus in vitro – a neuroanatomical tract tracing technique for the analysis of local fiber tracts in human brain. J. Neurosci. Methods 120, 95–103, http://dx.doi.org/10.1016/S0165-0270(02)00187-5.

Gefen, T., Peterson, M., Papastefan, S.T., Martersteck, A., Whitney, K., Rademaker, A., Bigio, E.H., Weintraub, S., Rogalski, E., Mesulam, M.-M., Geula, C., 2015. Morphometric and histologic substrates of cingulate integrity in elders with exceptional memory capacity. J. Neurosci. 35, 1781–1791, http://dx.doi.org/10.1523/JNEUROSCI.2998-14.2015.

Glantz, L.A., Lewis, D.A., 2000. Decreased dendritic spine density on prefrontal cortical pyramidal neurons in schizophrenia. Arch. Gen. Psychiatry 57, 65–73, http://dx.doi.org/10.1001/archpsyc.57.1.65.

Gomez-Nicola, D., Suzzi, S., Vargas-Caballero, M., Fransen, N.L., Al-Malki, H., Cebrian-Silla, A., Garcia-Verdugo, J.M., Riecken, K., Fehse, B., Perry, V.H., 2014. Temporal dynamics of hippocampal neurogenesis in chronic neurodegeneration. Brain 137, 2312–2328, http://dx.doi.org/10.1093/brain/awu155.

Hales, C.M., Dammer, E.B., Diner, I., Yi, H., Seyfried, N.T., Gearing, M., Glass, J.D., Montine, T.J., Levey, A.I., Lah, J.J., 2014. Aggregates of small nuclear ribonucleic acids (snRNAs) in Alzheimer's disease. Brain Pathol. 24, 344–351, http://dx.doi.org/10.1111/bpa.12133.

Hayashi-Takagi, A., Takaki, M., Graziane, N., Seshadri, S., Murdoch, H., Dunlop, A.J., Makino, Y., Seshadri, A.J., Ishizuka, K., Srivastava, D.P., Xie, Z., Baraban, J.M., Houslay, M.D., Tomoda, T., Brandon, N.J., Kamiya, A., Yan, Z., Penzes, P., Sawa, A., 2010. Disrupted-in-Schizophrenia 1 (DISC1) regulates spines of the glutamate synapse via Rac1. Nat. Neurosci. 13, 327–332, http://dx.doi.org/10.1038/nn.2487.

Hukkanen, V., Röyttä, M., 1987. Autolytic changes of human white matter: an electron microscopic and electrophoretic study. Exp. Mol. Pathol. 46, 31–39, http://dx.doi.org/10.1016/0014-4800(87)90028-1.

Ishizuka, K., Kamiya, A., Oh, E.C., Kanki, H., Seshadri, S., Robinson, J.F., Murdoch, H., Dunlop, A.J., Kubo, K., Furukori, K., Huang, B., Zeledon, M., Hayashi-Takagi, A., Okano, H., Nakajima, K., Houslay, M.D., Katsanis, N., Sawa, A., 2011. DISC1-dependent switch from progenitor proliferation to migration in the developing cortex. Nature 473, 92–96, http://dx.doi.org/10.1038/nature09859.

Kamiya, A., Kubo, K., Tomoda, T., Takaki, M., Youn, R., Ozeki, Y., Sawamura, N., Park, U., Kudo, C., Okawa, M., Ross, C.A., Hatten, M.E., Nakajima, K., Sawa, A., 2005. A schizophrenia-associated mutation of DISC1 perturbs cerebral cortex development. Nat. Cell Biol. 7, 1167–1178, http://dx.doi.org/10.1038/ncb1328.

Kulkarni, V.A., Firestein, B.L., 2012. The dendritic tree and brain disorders. Mol. Cell. Neurosci. 50, 10–20, http://dx.doi.org/10.1016/j.mcn.2012.03.005.

Lim, C., Mufson, E.J., Kordower, J.H., Blume, H.W., Madsen, J.R., Saper, C.B., 1997. Connections of the hippocampal formation in humans. 1. The Mossy fiber pathway. 2. The end-folial fiber pathway. J. Comp. Neurol. 385, 352–371.

Liu, X.-B., Schumann, C.M., 2014. Optimization of electron microscopy for human brains with long-term fixation and fixed-frozen sections. Acta Neuropathol. Commun. 2, 42, http://dx.doi.org/10.1186/2051-5960-2-42.

Luft, J.H., 1961. Improvements in epoxy resin embedding methods. J. Biophys. Biochem. Cytol. 9, 409–414.

Mason, J.T., O'Leary, T.J., 1991. Effects of formaldehyde fixation on protein secondary structure: a calorimetric and infrared spectroscopic investigation. J. Histochem. Cytochem. 39, 225–229, http://dx.doi.org/10.1177/39.2.1987266.

Millar, J.K., Wilson-Annan, J.C., Anderson, S., Christie, S., Taylor, M.S., Semple, C.A., Devon, R.S., St Clair, D.M., Muir, W.J., Blackwood, D.H., Porteous, D.J., 2000. Disruption of two novel genes by a translocation co-segregating with schizophrenia. Hum. Mol. Genet. 9, 1415–1423, http://dx.doi.org/10.1093/hmg/9.9.1415.

Miyoshi, K., Honda, A., Baba, K., Taniguchi, M., Oono, K., Fujita, T., Kuroda, S., Katayama, T., Tohyama, M., 2003. Disrupted-In-Schizophrenia 1, a candidate gene for schizophrenia, participates in neurite outgrowth. Mol. Psychiatry 8, 685–694, http://dx.doi.org/10.1038/sj.mp.4001352.

Nimchinsky, E.A., Vogt, B.A., Morrison, J.H., Hof, P.R., 1995. Spindle neurons of the human anterior cingulate cortex. J. Comp. Neurol. 355, 27–37, http://dx.doi.org/10.1002/cne.903550106.

O'Leary, T.J., Fowler, C.B., Evers, D.L., Mason, J.T., 2009. Protein fixation and antigen retrieval: chemical studies. Biotech. Histochem. 84, 217–221, http://dx.doi.org/10.3109/10520290903039086.

Ozeki, Y., Tomoda, T., Kleiderlein, J., Kamiya, A., Bord, L., Fujii, K., Okawa, M., Yamada, N., Hatten, M.E., Snyder, S.H., Ross, C.A., Sawa, A., 2003. Disrupted-in-Schizophrenia-1 (DISC-1): mutant truncation prevents binding to NudE-like (NUDEL) and inhibits neurite outgrowth. Proc. Natl. Acad. Sci. U.S.A. 100, 289–294, http://dx.doi.org/10.1073/pnas.0136913100.

Raghanti, M.A., Spurlock, L.B., Robert Treichler, F., Weigel, S.E., Stimmelmayr, R., Butti, C., Hans Thewissen, J.G.M., Hof, P.R., 2015. An analysis of von Economo neurons in the cerebral cortex of cetaceans, artiodactyls, and perissodactyls. Brain Struct. Funct. 220, 2303–2314, http://dx.doi.org/10.1007/s00429-014-0792-y.

Rait, V.K., Xu, L., O'Leary, T.J., Mason, J.T., 2004. Modeling formalin fixation and antigen retrieval with bovine pancreatic RNase A II. Interrelationship of cross-linking, immunoreactivity, and heat treatment. Lab. Invest. 84, 300–306, http://dx.doi.org/10.1038/labinvest.3700041.

Reynolds, E.S., 1963. The use of lead citrate at high pH as an electron-opaque stain in electron microscopy. J. Cell Biol. 17, 208–212, http://dx.doi.org/10.1083/jcb.17.1.208.

Richardson, K.C., Jarett, L., Finke, E.H., 1960. Embedding in epoxy resins for ultrathin sectioning in electron microscopy. Stain Technol. 35, 313–323, http://dx.doi.org/10.3109/10520296009114754.

Sabatini, D.D., Bensch, K., Barrnett, R.J., 1963. Cytochemistry and electron microscopy. The preservation of cellular ultrastructure and enzymatic activity by aldehyde fixation. J. Cell Biol. 17, 19–58, http://dx.doi.org/10.1083/jcb.17.1.19.

Schneider, C.A., Rasband, W.S., Eliceiri, K.W., 2012. NIH Image to ImageJ: 25 years of image analysis. Nat. Methods 9, 671–675, http://dx.doi.org/10.1038/nmeth.2089.

Seeley, W.W., Carlin, D.A., Allman, J.M., Macedo, M.N., Bush, C., Miller, B.L., DeArmond, S.J., 2006. Early frontotemporal dementia targets neurons unique to apes and humans. Ann. Neurol. 60, 660–667, http://dx.doi.org/10.1002/ana.21055.

Simms, M.L., Kemper, T.L., Timbie, C.M., Bauman, M.L., Blatt, G.J., 2009. The anterior cingulate cortex in autism: heterogeneity of qualitative and quantitative cytoarchitectonic features suggests possible subgroups. Acta Neuropathol. 118, 673–684, http://dx.doi.org/10.1007/s00401-009-0568-2.

Stimpson, C.D., Tetreault, N.A., Allman, J.M., Jacobs, B., Butti, C., Hof, P.R., Sherwood, C.C., 2011. Biochemical specificity of von economo neurons in hominoids. Am. J. Hum. Biol. 23, 22–28, http://dx.doi.org/10.1002/ajhb.21135.

Uranova, N.A., Vikhreva, O.V., Rachmanova, V.I., Orlovskaya, D.D., 2011. Ultrastructural alterations of myelinated fibers and oligodendrocytes in the prefrontal cortex in schizophrenia: a postmortem morphometric study. Schizophr. Res. Treatment 2011, 1–13, http://dx.doi.org/10.1155/2011/325789.

Von Economo, C., 1926. Eine neue Art Spezialzellen des Lobus cinguli und Lobus insulae. Zeitschrift für die gesamte Neurol. und Psychiatr. 100, 706–712.

Wadsworth, P.F., Jones, H.B., Cavanagh, J.B., 1995. The topography, structure and incidence of mineralized bodies in the basal ganglia of the brain of cynomolgus monkeys (*Macaca fascicularis*). Lab. Anim. 29, 276–281.

Watson, K.K., Jones, T.K., Allman, J.M., 2006. Dendritic architecture of the von Economo neurons. Neuroscience 141, 1107–1112, http://dx.doi.org/10.1016/j.neuroscience.2006.04.084.

Zhang, S., Qi, J., Li, X., Wang, H.-L., Britt, J.P., Hoffman, A.F., Bonci, A., Lupica, C.R., Morales, M., 2015. Dopaminergic and glutamatergic microdomains in a subset of rodent mesoaccumbens axons. Nat. Neurosci. 18, 386–392, http://dx.doi.org/10.1038/nn.3945.